Escola de Primavera de Transição e Turbulência
Blumenau 2020

ABCM Associação Brasileira de Engenharia e Ciências Mecânicas

12th Spring School on Transition and Turbulence
September 21st-25th, 2020, Blumenau, SC, Brazil

# ETT-2020-0118
# NUMERICAL SIMULATION OF BARCHAN DUNES IN A TURBULENT CHANNEL FLOW

**Carlos A. Alvarez**
**Erick M. Franklin**
School of Mechanical Engineering, University of Campinas - UNICAMP, Rua Mendeley, 200, Campinas, SP, Brazil
calvarez@fem.unicamp.br, franklin@fem.unicamp.br

***Abstract.*** *Barchan dunes are characterized by a crescentic shape and can be found in rivers, terrestrial deserts and other planetary environments. These bedforms present different scales according to the environment they are in, their length scale varying from the decimeter under water to the kilometer on Mars. Depending on the nature of the entraining fluid the transport of grains presents significant differences so that the growth of this kind of dunes rests to be fully understood. Aquatic barchans have smaller length and time scales, so they are the ideal object to characterize the growth of these bedforms. In this work, we computed the bed evolution by using the computational fluid dynamics - discrete element method, where we coupled the discrete element method with large eddy simulation. We obtained the resultant force acting on each grain, which has not been previously measured nor computed. Our results show that the present method is appropriate for numerical computations of bedforms, opening new possibilities for accessing data that are not available from current experiments. This paper is based on C. A. Alvarez and E. M. Franklin, Phys. Rev. E 101, 012905 (2020) and reproduces many of its parts.*

***Keywords:*** *grains, bed load, barchan dunes, large eddy simulation, discrete element method*

## 1. INTRODUCTION

Barchan dunes can be found in highly diverse environments such as rivers, oil pipelines, terrestrial deserts, and even other planetary environments like Mars and Venus (Bagnold, 1941; Hersen *et al.*, 2002; Claudin and Andreotti, 2006; Parteli and Herrmann, 2007). Barchans are usually formed when grains are transported as bed load by a one-directional fluid flow, and they are characterized by a crescentic shape with horns pointing downstream (Bagnold, 1941; Hersen *et al.*, 2002). This shape presents different scales according to the environment the barchans are in. Aquatic dunes, have smaller scales (Franklin and Charru, 2009, 2011) than Aeolian and Martian dunes (Claudin and Andreotti, 2006; Parteli and Herrmann, 2007). For this reason, many studies carried out experiments in water channels in order to obtain the length and time scales of barchans (Hersen *et al.*, 2002; Franklin and Charru, 2011; Alvarez and Franklin, 2017) and typical trajectories and velocities of moving grains (Alvarez and Franklin, 2018b, 2019). In previous works (Alvarez and Franklin, 2017, 2018b), we presented the characteristic times $0.5t_c$ and $2.5t_c$ for the growth and equilibrium of barchans, respectively, where $t_c$ is a proposed time scale computed as the length of the bedform divided by its celerity. Numerical simulations are another way to investigate the dynamics of these bedforms. The first numerical works computing large-scale dunes employed continuum models for the grains (Sauermann *et al.*, 2001; Herrmann and Sauermann, 2000; Kroy *et al.*, 2002a,b, 2005; Schwämmle and Herrmann, 2005; Parteli *et al.*, 2014) and considered that saltation was the mode of entrainment, occurring mainly in the longitudinal direction, with some transverse diffusion. However, the transverse displacements of grains in the subaqueous case are, on average, comparable to the longitudinal ones, as shown recently by Alvarez and Franklin (2018b, 2019) and Alvarez (2020), a situation different from what is generally conjectured for the Aeolian and Martian cases. Khosronejad and Sotiropoulos (2017) coupled a large eddy simulation (LES) model for the water and water-suspension mixture with a continuum model involving the entrainment and Exner equations for the granular bed, obtaining morphological characteristics of bedforms, but with their model, it is not possible to access data at the grain scale.

Coupling the computational fluid dynamics with the discrete element method (CFD-DEM) it is possible to capture the main features of bed load (Schmeeckle, 2014; Kidanemariam and Uhlmann, 2014b; Liu *et al.*, 2016; Sun and Xiao, 2016; Pähtz and Durán, 2017) and bedforms (Kidanemariam and Uhlmann, 2014a, 2017). Schmeeckle (2014) presented a model coupling DEM with LES based on the open source codes CFDEM (Goniva *et al.*, 2012) (www.cfdem.com), OpenFOAM (www.openfoam.org), and LIGGGHTS (Kloss and Goniva, 2010; Berger *et al.*, 2015), that was used to compute sand transport by water. His results showed that bed-load grains move generally in contact with the bed and that saltation is of lesser importance in the subaqueous case, with most of the grains being dislodged directly by the water flow.

Pähtz and Durán (2017) investigated numerically the mechanisms of the entrainment of grains by using DEM coupled with Reynolds-averaged Navier-Stokes equations (RANS). The authors defined that the grains can be transported by two mechanisms: directly by the fluid (fluid entrainment) and by particle-bed impacts (impact entrainment). However, for a given range of flows, Schmeeckle (2014) and Pähtz and Durán (2017) present contrasting results with respect to grain entrainment.

In the last years, some studies, investigating the growth of bedforms in the subaqueous case, have employed direct numerical simulations (DNS) for the fluid and DEM for the grains (Kidanemariam and Uhlmann, 2014a,b, 2017). This proposed methodology is currently the most accurate, avoiding the use of turbulence models for the fluid, capturing all the scales of turbulence down to the Kolmogorov scale, and fully solving the flow around each grain. However, the computational cost is exceedingly high, so that the time required for obtaining developed bedforms is seldom reached (Colombini, 2014). In this sense, the LES method, although needing subgrid turbulence models, can be an excellent choice to compute the flow around bedforms including recirculation regions with a much lower computational cost than DNS. Although some numerical investigations succeeded in capturing the formation of subaqueous barchans, they did not report detailed measurements at the grain scale. In addition, the role of water in the direct entrainment of grains is still a subject of debate. In this work, we reproduce numerically the evolution of the bedform morphology and we found the resultant forces acting on grains, being the latter not accessible from reported experiments. Our results show that the used method is appropriate to numerical computations of subaqueous barchan, opening new possibilities for other studies on aquatic bedforms. This paper is based on C. A. Alvarez and E. M. Franklin, Phys. Rev. E 101, 012905 (2020) and reproduces many of its parts.

## 2. NUMERICAL SETUP

Our numerical investigation was conducted with CFD-DEM, where the dynamics of each individual particle was computed by DEM (Cundall and Strack, 1979) using the resulting forces and torques on each particle, the fluid flow was computed by LES, and momentum coupling was made between solids and fluid. The solid particles and the fluid are treated in the Lagrangian and the Eulerian frameworks, respectively.

We used the open source code CFDEM (Goniva *et al.*, 2012) (www.cfdem.com) for our CFD-DEM computations. CFDEM links the open source code OpenFOAM, which computes the fluid flow based on the finite volume method (FVM), with the open source code LIGGGHTS (Kloss and Goniva, 2010; Berger *et al.*, 2015), which computes the dynamics of grains. Concerning the grains, we considered a Hertzian model for which we set up the coefficient of restitution $e$ as approximately 0.1 because collisions are expected to be viscous damped (Schmeeckle, 2014). The friction coefficient $\mu_{fr}$ was considered as 0.6 (Schmeeckle, 2014; Liu *et al.*, 2016), and Young's modulus $E$ and the Poisson ratio $\sigma$ were obtained from Tsuji *et al.* (1992, 1993). Young's modulus used in the simulations is considerably smaller than real values in order to reduce the DEM time step without affecting significantly the numerical outputs (Tsuji *et al.*, 1993). The DEM parameters are the same as those of Alvarez and Franklin (2020). For the fluid, we used LES with subgrid stresses given by the wall-adapting local eddy-viscosity (WALE) model (Nicoud and Ducros, 1999). The domain was set to $0.3 \times 0.05 \times 0.16$ m divided into 150, 150 and 160 segments in the streamwise, $x$, wall-normal, $y$, and spanwise, $z$, directions, respectively. The dimensions in $y = 2\delta$ and $z$ directions are the same as those of the previous experiments (Alvarez and Franklin, 2017, 2018a,b, 2019). The segments in the $x$ and $z$ directions are uniform in size, whereas in the $y$ direction they are unevenly spaced. Details of the model description, and the grid and Reynolds numbers employed in our simulations can be found in Alvarez and Franklin (2020).

Prior to CFD-DEM simulations, single phase flows were computed in the computational domain, corresponding to a rectangular cross-sectional channel. Periodic conditions were considered in streamwise and spanwise directions, and the final realization was saved to be used as the fluid initial condition for the CFD-DEM simulations with grains. Also prior to starting the simulations, the water flow was set to zero velocity and the grains were poured from above, falling freely in water at a longitudinal location 0.05 m from the domain inlet and centered in the transverse direction. After a period for the grains to settle, we obtained an initially conical pile with radius $R = 0.025$ m, similar to Alvarez and Franklin (2017, 2018a,b, 2019), and the center at 0.05 m from the domain inlet. Once the initial condition for the grains was reached, we imposed the final realization of the single-phase LES computations as the initial condition for water. The boundary conditions for the fluid were impermeability and no-slip conditions at the top and bottom walls of the channel, and periodic conditions in the longitudinal and transverse directions. The boundary conditions for the solid particles were solid walls at the top and bottom walls, free exit at the outlet, and no mass entering at the inlet, so that the barchan decreased slightly in size while migrating, in the same manner as in Alvarez and Franklin (2017, 2018b). Figure 1 shows a layout of the computational domain.

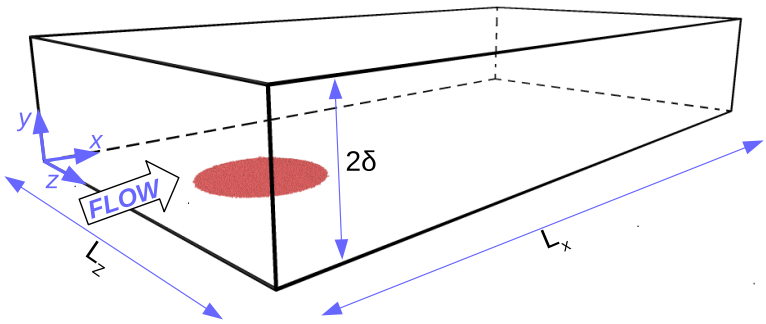


Figure 1. Layout of the computational setup. In the simulations, $L_x$ = 0.3 m, $2\delta$ = 0.05 m and $L_z$ = 0.16 m. (Figure extracted from Alvarez and Franklin (2020))

## 3. RESULTS AND DISCUSSION

### 3.1 Single water flow

Computations of single-phase channel flows were necessary to be used as the initial condition for the simulations with solid particles. Figure 2 shows a channel lateral view containing the streamwise velocity fluctuation along $y$, at a certain time $t$, from the single-water simulation. In order to evaluate our LES computations, the single phase simulations for $Re_*$ = 420 were compared with the DNS results of Moser *et al.* (1999) for $Re_*$ = 395. For that, we averaged 1,000 velocity fields in time (the last of 3,000 fields) and in the $x$ and $z$ directions, obtaining the profile of mean velocity, which were compared afterward with Moser *et al.* (1999).

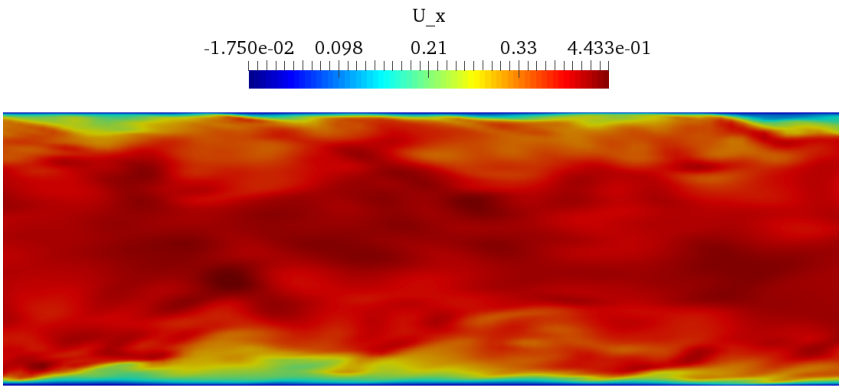


Figure 2. Streamwise velocity fluctuation along $y$ at a certain time $t$ from the single-water simulation. The lateral view corresponds to the full size of the channel in the $y$ direction, but only a portion along $x$ direction. The flow is from left to right, the color bar is m/s and $Re = 1.82\times10^4$.

Figures 3 present the profile of the longitudinal component of the mean velocity in the traditional log-normal scales, normalized by the inner scales, where solid lines correspond to the present LES results and dashed lines to the DNS results of Moser *et al.* (1999). In this figure, $u$ is the longitudinal component of the mean velocity, $u^+ = u/u_*$, with $u_*$ being the shear velocity. Figure 3 presents also the law of the wall with $\kappa$ = 0.41 and $B$ = 5.2.

In Fig. 3 we can observe that in the viscous region the mean profile obtained with LES shows a good agreement with both the law of the wall and DNS results of Moser *et al.* (1999), while in the overlap region LES results are shifted upwards with the same slope when compared with both the law of the wall and DNS. We consider, however, that the present results are adequate for the purpose of initial conditions for simulations with bed load, because two-dimensional measurements, with particle image velocimetry (PIV), in a channel with the same dimensions provided similar results (Franklin *et al.*, 2014; Cúñez *et al.*, 2018).

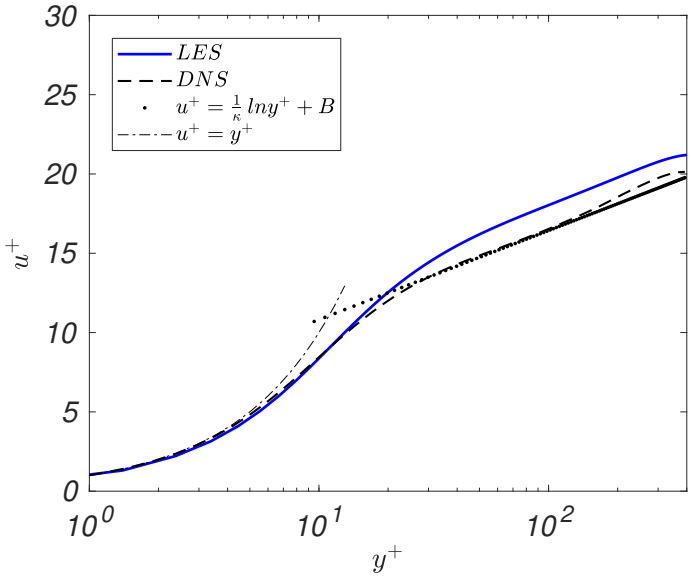


Figure 3. Single-phase flow in the channel. Profile of the longitudinal component of the mean velocity $u$ in the traditional log-normal scales, normalized by the inner scales. Figure presents also the law of the wall with $\kappa$ = 0.41 and $B$ = 5.2. (Figure extracted from Alvarez and Franklin (2020))

### 3.1.1 Forces on grains

The present simulations provide us with the resultant force acting on each grain, i.e., $\vec{F}_p = \vec{F}_{fp} + \vec{F}_c + m_p\vec{g}$, where $\vec{F}_{fp}$, $\vec{F}_c$, and $m_p\vec{g}$ are the resultant of fluid forces on grains, the resultant of contact forces between solids, and the particle weight, respectively. This information is difficult to access experimentally, and it is not available from current experiments.

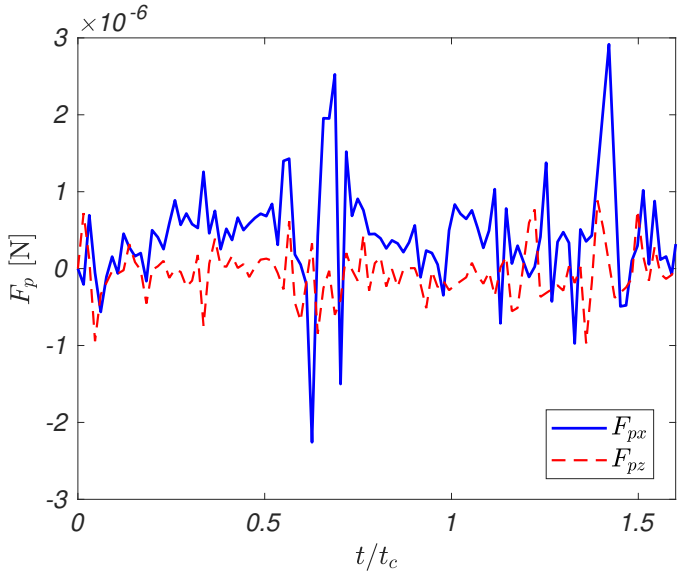


Figure 4. Longitudinal and transverse components of the resultant force on a grain, $F_{px}$ and $F_{pz}$, respectively, as a function of time. This specific grain was entrained from an upstream region toward the crest, and $Re = 1.47\times10^4$. (Figure extracted from Alvarez and Franklin (2020))

Figure 4 presents the resultant force on a tracked grain as it was entrained from an upstream region until the dune crest, and it is representative of the resultant force acting on grains migrating toward the crest. In Fig. 4, the solid blue line corresponds to the longitudinal component of the force, $F_{px}$, and the dashed red line to the transverse component of the force, $F_{pz}$. We observe that the grain experiences a varying force, in the transverse direction the instantaneous

values varying around a zero average, while in the longitudinal direction the force has a positive average, with high peaks occurring in some occasions. These peaks are much higher than the mean value (in Fig. 4, the highest peak is one order of magnitude greater than the mean value). It is interesting to note that this specific grain took a time slightly longer than $1.5t_c$ to reach the dune crest, with the highest peak occurring just before reaching the crest.

Figures 5(a) and 5(b) present, respectively, PDFs of the longitudinal and transverse components of the resultant force acting on each grain crossing a given barchan cross section. Figure 5 shows that the resultant force acting on each grain has a longitudinal component that attains higher values on upstream regions and decays toward the crest, with a slightly broader distribution upstream, while the transverse component is always peaked at zero, also with a broader distribution upstream. Although the longitudinal component of the resultant force is lower at the crest, the granular flux increases toward the crest (Alvarez and Franklin, 2020) due probably to the grain inertia. The results on the resultant force, which have until now been only conjectured, help to explain the mechanism of upstream erosion and crest deposition that exists on barchan dunes.

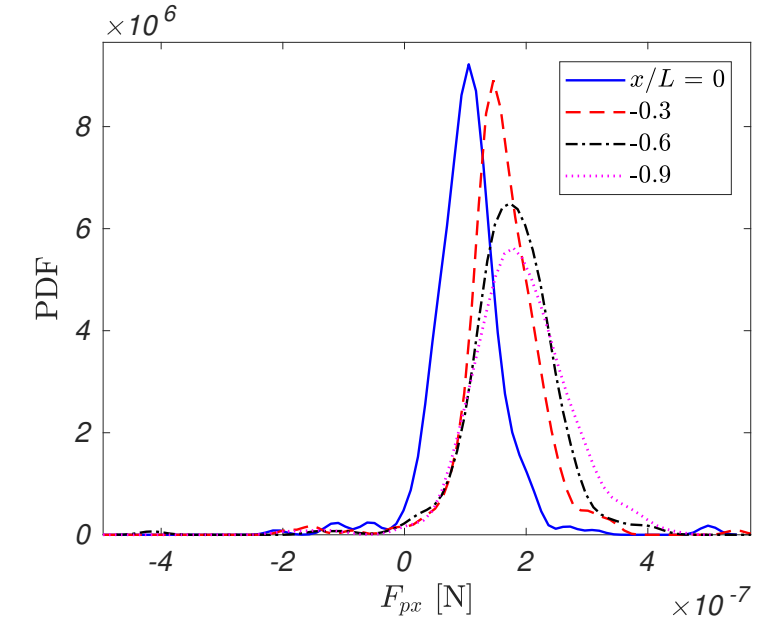


(a)

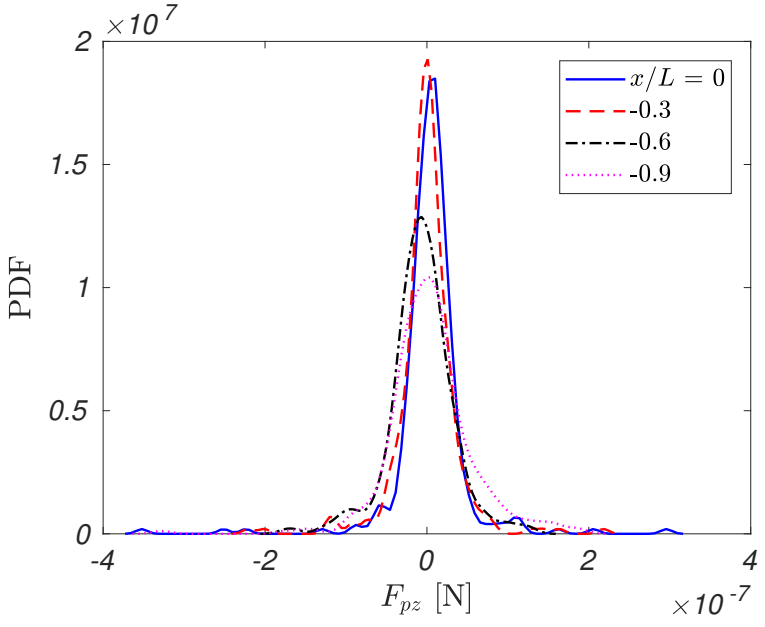


(b)

Figure 5. PDFs of (a) the longitudinal and (b) transverse components of the resultant force acting on each grain crossing a given barchan cross section. The longitudinal positions of each considered cross section ($x$ planes) are listed in the figure key and $Re = 1.47\times10^4$. (Figure extracted from Alvarez and Franklin (2020))

## 4. CONCLUSIONS

This work investigated numerically the formation and evolution of single barchans by using the computational fluid dynamics - discrete element method (CFD-DEM), where the DEM was coupled with the large eddy simulation (LES). The simulations were performed in a closed-conduit channel where initially conical heaps evolved to single barchans under the action of a turbulent water flow. The profile of the longitudinal component of the mean velocity, obtained by using LES, showed good agreement with both the law of the wall and DNS results, being adequate for the purpose of initial conditions for simulations with bed load. We also obtained the resultant force acting on each grain, which has not been previously measured nor computed. For this force, we showed that its longitudinal component attains higher values on upstream regions and decays toward the crest. These results help to explain the mechanism of upstream erosion and crest deposition that exists on barchan dunes. The good agreement between the numerical and experimental results shows that the present method is appropriate for numerical computations of bedforms, opening new possibilities for accessing data not available from current experiments.

## 5. ACKNOWLEDGEMENTS

C.A.A. is grateful to SENESCYT (Grant No.2013-AR2Q2850) and to CNPq (Grant No. 140773/2016-9). E.M.F. is grateful to FAPESP (Grant No. 2018/14981-7) and to CNPq (Grant No. 400284/2016-2) for the financial support provided. C.A.A. is also grateful to Western University and the Emerging Leaders in the Americas Program, Global Affairs Canada. The authors would like to thank Prof. J. M. Floryan from Western University, Canada, for helpful discussions. SHARCNET (www.sharcnet.ca) provided part of computational resources used in the project.

## 6. REFERENCES

Alvarez, C.A., 2020. "Genesis and formation of subaqueous barchan dunes: from a morphological characterization to a description at the grain scale". *Ph.D. Thesis, University of Campinas, Brazil*.

Alvarez, C.A. and Franklin, E.M., 2017. "Birth of a subaqueous barchan dune". *Physical Review E*, Vol. 96, No. 6, p. 062906.

Alvarez, C.A. and Franklin, E.M., 2018a. "Experimental study on the formation of subaqueous barchan dunes in closed conduits". In *Experimental Fluid Mechanics 2017. EPJ Web of Conferences*. Vol. 180, p. 02002.

Alvarez, C.A. and Franklin, E.M., 2018b. "Role of transverse displacements in the formation of subaqueous barchan dunes". *Physical Review Letters*, Vol. 121, No. 16, p. 164503.

Alvarez, C.A. and Franklin, E.M., 2019. "Horns of subaqueous barchan dunes: A study at the grain scale". *Physical Review E*, Vol. 100, No. 4, p. 042904.

Alvarez, C.A. and Franklin, E.M., 2020. "Shape evolution of numerically obtained subaqueous barchans". *Physical Review E*, Vol. 101, No. 1, p. 012905.

Bagnold, R.A., 1941. *The Physics of Blown Sand and Desert Dunes*. Chapman and Hall, London.

Berger, R., Kloss, C., Kohlmeyer, A. and Pirker, S., 2015. "Hybrid parallelization of the LIGGGHTS open-source DEM code". *Powder Technology*, Vol. 278, pp. 234–247.

Claudin, P. and Andreotti, B., 2006. "A scaling law for aeolian dunes on Mars, Venus, Earth, and for subaqueous ripples". *Earth and Planetary Science Letters*, Vol. 252, No. 1-2, pp. 30–44.

Colombini, M., 2014. "A decade's investigation of the stability of erodible stream beds". *Journal of Fluid Mechanics*, Vol. 756, pp. 1–4.

Cundall, P.A. and Strack, O.D., 1979. "A discrete numerical model for granular assemblies". *Géotechnique*, Vol. 29, No. 1, pp. 47–65.

Cúñez, F.D., de Oliveira, G.V.G. and Franklin, E.M., 2018. "Turbulent channel flow perturbed by triangular ripples". *Journal of the Brazilian Society of Mechanical Sciences and Engineering*, Vol. 40, No. 3, p. 138.

Franklin, E.M. and Charru, F., 2011. "Subaqueous barchan dunes in turbulent shear flow. Part 1. Dune motion". *Journal of Fluid Mechanics*, Vol. 675, pp. 199–222.

Franklin, E.M., de Figueiredo, F.T. and Rosa, E.S., 2014. "The feedback effect caused by bed load on a turbulent liquid flow". *Journal of the Brazilian Society of Mechanical Sciences and Engineering*, Vol. 36, No. 4, pp. 725–736.

Franklin, E.M. and Charru, F., 2009. "Morphology and displacement of dunes in a closed-conduit flow". *Powder Technology*, Vol. 190, No. 1-2, pp. 247–251.

Goniva, C., Kloss, C., Deen, N.G., Kuipers, J.A.M. and Pirker, S., 2012. "Influence of rolling friction on single spout fluidized bed simulation". *Particuology*, Vol. 10, No. 5, pp. 582–591.

Herrmann, H.J. and Sauermann, G., 2000. "The shape of dunes". *Physica A: Statistical Mechanics and its Applications*, Vol. 283, No. 1-2, pp. 24–30.

Hersen, P., Douady, S. and Andreotti, B., 2002. "Relevant length scale of barchan dunes". *Physical Review Letters*, Vol. 89, No. 26, p. 264301.

Khosronejad, A. and Sotiropoulos, F., 2017. "On the genesis and evolution of barchan dunes: morphodynamics". *Journal of Fluid Mechanics*, Vol. 815, pp. 117–148.

Kidanemariam, A.G. and Uhlmann, M., 2014a. "Direct numerical simulation of pattern formation in subaqueous sediment". *Journal of Fluid Mechanics*, Vol. 750.

Kidanemariam, A.G. and Uhlmann, M., 2014b. "Interface-resolved direct numerical simulation of the erosion of a sediment bed sheared by laminar channel flow". *International Journal of Multiphase Flow*, Vol. 67, pp. 174–188.

Kidanemariam, A.G. and Uhlmann, M., 2017. "Formation of sediment patterns in channel flow: minimal unstable systems and their temporal evolution". *Journal of Fluid Mechanics*, Vol. 818, pp. 716–743.

Kloss, C. and Goniva, C., 2010. "LIGGGHTS: A new open source discrete element simulation software". In *Proceedings of 5th International Conference on Discrete Element Methods*. London, UK.

Kroy, K., Fischer, S. and Obermayer, B., 2005. "The shape of barchan dunes". *Journal of Physics: Condensed Matter*, Vol. 17, No. 14, p. S1229.

Kroy, K., Sauermann, G. and Herrmann, H.J., 2002a. "Minimal model for aeolian sand dunes". *Physical Review E*, Vol. 66, No. 3, p. 031302.

Kroy, K., Sauermann, G. and Herrmann, H.J., 2002b. "Minimal model for sand dunes". *Physical Review Letters*, Vol. 88, No. 5, p. 054301.

Liu, D., Liu, X., Fu, X. and Wang, G., 2016. "Quantification of the bed load effects on turbulent open-channel flows". *Journal of Geophysical Research: Earth Surface*, Vol. 121, No. 4, pp. 767–789.

Moser, R.D., Kim, J. and Mansour, N.N., 1999. "Direct numerical simulation of turbulent channel flow up to Re$\tau$= 590". *Physics of Fluids*, Vol. 11, No. 4, pp. 943–945.

Nicoud, F. and Ducros, F., 1999. "Subgrid-scale stress modelling based on the square of the velocity gradient tensor". *Flow, Turbulence and Combustion*, Vol. 62, No. 3, pp. 183–200.

Pähtz, T. and Durán, O., 2017. "Fluid forces or impacts: What governs the entrainment of soil particles in sediment transport mediated by a Newtonian fluid?" *Physical Review Fluids*, Vol. 2, No. 7, p. 074303.

Parteli, E.J.R., Durán, O., Bourke, M.C., Tsoar, H., Pöschel, T. and Herrmann, H., 2014. "Origins of barchan dune asymmetry: Insights from numerical simulations". *Aeolian Research*, Vol. 12, pp. 121–133.

Parteli, E.J.R. and Herrmann, H.J., 2007. "Dune formation on the present Mars". *Physical Review E*, Vol. 76, No. 4, p. 041307.

Sauermann, G., Kroy, K. and Herrmann, H.J., 2001. "Continuum saltation model for sand dunes". *Physical Review E*, Vol. 64, No. 3, p. 031305.

Schmeeckle, M.W., 2014. "Numerical simulation of turbulence and sediment transport of medium sand". *Journal of Geophysical Research: Earth Surface*, Vol. 119, No. 6, pp. 1240–1262.

Schwämmle, V. and Herrmann, H., 2005. "A model of barchan dunes including lateral shear stress". *The European Physical Journal E*, Vol. 16, No. 1, pp. 57–65.

Sun, R. and Xiao, H., 2016. "SediFoam: A general-purpose, open-source CFD-DEM solver for particle-laden flow with emphasis on sediment transport". *Computers & Geosciences*, Vol. 89, pp. 207–219.

Tsuji, Y., Kawaguchi, T. and Tanaka, T., 1993. "Discrete particle simulation of two-dimensional fluidized bed". *Powder Technology*, Vol. 77, No. 1, pp. 79–87.

Tsuji, Y., Tanaka, T. and Ishida, T., 1992. "Lagrangian numerical simulation of plug flow of cohesionless particles in a horizontal pipe". *Powder Technology*, Vol. 71, No. 3, pp. 239–250.

## 7. RESPONSIBILITY NOTICE

The authors are the only responsible for the printed material included in this paper.